

DETC2007-35330

DEGREE OPERATIONS ON PERIODIC SURFACES

Yan Wang

Department of Industrial Engineering & Management Systems
University of Central Florida
Orlando, FL 32816

ABSTRACT

In previous work, a periodic surface model for computer-aided nano-design (CAND) was developed. This implicit surface model can construct Euclidean and hyperbolic nano geometries parametrically and represent morphologies of particle aggregates and polymers. In this paper, we study the characteristics of degree elevation and reduction based on a generalized periodic surface model. Methods of degree elevation and reduction operations are developed in order to support multi-resolution representation and model exchange.

1. INTRODUCTION

Computer-aided nano-design (CAND) is an extension of computer based engineering design traditionally at bulk scales to nano scales. The general target of modeling and simulation in nanomaterial design is to search stable and realizable structures and conformations with the minimal total system energy. Geometry optimization is the central theme in nanoscale simulations. For the widely used local search algorithms, simulation results are sensitively dependent on the initial conformation. Methods that allow for the efficient construction of initial geometries that are reasonably close to global optimal solutions are important to improve both convergence rate and accuracy of prediction. Thus, enabling efficient structural description is one of the key research issues in CAND.

Traditional boundary-based parametric solid modeling methods do not support efficient construction of complex and dynamic nano-scale geometries due to some special characteristics at the low levels. For instance, there are no clear-cut boundaries of substances among atoms and molecules. The quantum-level uncertainty principle indicates the impossibility of specifying the precise momentum and position of a particle simultaneously. Volume packing of different atoms with clouds of correlated electrons is the central design problem at the atomic scale. Non-deterministic geometries and topologies at the molecular scale are the manifestations of thermodynamic and kinetic properties.

Parametric modeling mechanisms of particle aggregates at the molecular scale are needed to support rapid construction and optimization of geometries. At the meso scale, super-porous structures with high surface-volume ratios in natural and man-made materials also need effective geometric descriptions. Providing nano engineers and scientists efficient and easy-to-use tools to create geometry conformations that have minimum energies is highly desirable in material design.

With the observation that hyperbolic surfaces exist in nature ubiquitously and periodic features are common in condensed materials, we recently proposed an implicit surface modeling approach, periodic surface, to represent geometric structures in nano scales [1, 2]. Periodic surfaces are either *loci* or *foci*. Loci surfaces are fictional continuous surfaces that pass through discrete particles in 3D space, whereas foci surfaces can be looked as isosurfaces of potential or density in which discrete particles are enclosed. The model allows for parametric construction from atomic scale to meso scale. Reconstruction of loci surfaces from crystals was also studied [3].

The ability to control the complexity of models is important for engineers during the nanomaterial design process. Flexible tools that allow for modifying design features locally and globally are essential. Degree elevation, which increases the complexity of models incrementally, and degree reduction, which decreases the complexity gradually, are two such mechanisms. They provide the basic controllability and enable multi-resolution representation of periodic surface models. They also enable model exchanges of similar surfaces at similar scales.

In this paper, we present the properties of degree elevation and reduction for periodic surfaces. Examples are used to illustrate three methods for degree elevation and one approach for degree reduction. In the remainder of the paper, Section 2 gives a brief overview of related work in molecular surface modeling. Section 3 describes the basis of the periodic surface model. Section 4 shows the three basic types of degree elevation, and Section 5 presents a method for degree reduction.

2. MOLECULAR SURFACE MODELING

For visualization purpose, there has been some research on molecular surface modeling to visualize molecular structures [4]. Lee and Richards [5] first introduced solvent-accessible surface, the locus of a probe rolling over Van der Waals surface, to represent boundary of molecules. Connolly [6] presented an analytical method to calculate the surface. Recently, Carson [7] represented molecular surfaces with B-spline wavelet. Edelsbrunner [8] described molecules with implicit-form skin surfaces. Bajaj et al. [9] represented solvent accessible surfaces by NURBS (non-uniform rational B-spline). Kim et al. [10] constructed NURBS molecular surfaces by the aid of Euclidean Voronoi diagrams. These research efforts concentrate on visualization of molecules, whereas construction support of molecular and atomic structures for design purpose is not considered. We recently proposed a periodic surface model to construct nano structures parametrically.

3. PERIODIC SURFACE

A periodic surface (PS) is generally defined as

$$\psi(\mathbf{r}) = \sum_{l=1}^L \sum_{m=1}^M \mu_{lm} \cos(2\pi\kappa_l(\mathbf{p}_m^T \cdot \mathbf{r})) = 0 \quad (1)$$

where κ_l is the *scale parameter*, $\mathbf{p}_m = [a_m, b_m, c_m, \theta_m]^T$ is a *basis vector*, such as one of

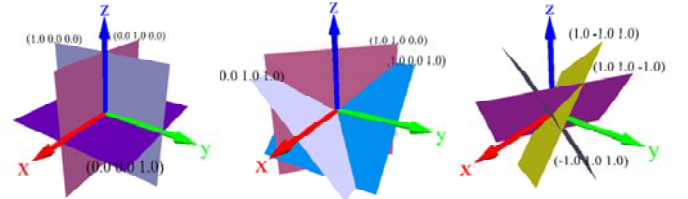
$$\{\mathbf{e}_0, \mathbf{e}_1, \mathbf{e}_2, \mathbf{e}_3, \mathbf{e}_4, \mathbf{e}_5, \mathbf{e}_6, \mathbf{e}_7, \mathbf{e}_8, \mathbf{e}_9, \mathbf{e}_{10}, \mathbf{e}_{11}, \dots\} = \quad (2)$$

$$\left\{ \begin{bmatrix} 0 \\ 0 \\ 0 \\ 1 \end{bmatrix}, \begin{bmatrix} 1 \\ 0 \\ 0 \\ 1 \end{bmatrix}, \begin{bmatrix} 0 \\ 1 \\ 0 \\ 1 \end{bmatrix}, \begin{bmatrix} 0 \\ 0 \\ 1 \\ 1 \end{bmatrix}, \begin{bmatrix} 1 \\ 1 \\ 0 \\ 1 \end{bmatrix}, \begin{bmatrix} 0 \\ 1 \\ 1 \\ 1 \end{bmatrix}, \begin{bmatrix} 1 \\ 1 \\ 1 \\ 1 \end{bmatrix}, \begin{bmatrix} -1 \\ 0 \\ 1 \\ 1 \end{bmatrix}, \begin{bmatrix} 0 \\ 1 \\ -1 \\ 1 \end{bmatrix}, \dots \right\},$$

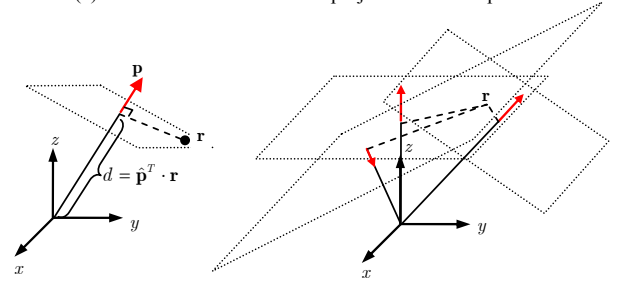
which represents a *basis plane* in the projective 3-space \mathbb{P}^3 , $\mathbf{r} = [x, y, z, w]^T$ is the location vector with homogeneous coordinates, and μ_{lm} is the *periodic moment*. We assume $w = 1$ throughout the paper if not explicitly specified. The *degree* of $\psi(\mathbf{r})$ in Eq. (1) is defined as the number of unique periodic

basis vectors in set $\{\mathbf{p}_m\}$, $\deg(\psi(\mathbf{r})) := |\{\mathbf{p}_m\}|$. The *scale* of $\psi(\mathbf{r})$ is defined as the number of unique scale parameters in set $\{\kappa_l\}$, $\text{sca}(\psi(\mathbf{r})) := |\{\kappa_l\}|$. In this paper, we assume the scale parameters are natural numbers ($\kappa_l \in \mathbb{N}$).

As illustrated in Figure 1, each basis vector represents a 2D subspaces in \mathbb{P}^3 . $d_m = \hat{\mathbf{p}}_m^T \cdot \mathbf{r} = \mathbf{p}_m^T \cdot \mathbf{r} / \|\mathbf{p}_m\|$ corresponding to the basis plane \mathbf{p}_m can be looked as a *projective distance* between the origin and the projective subspace where \mathbf{r} resides in. The projective distance is negative when the normal direction of the subspace is towards the origin, otherwise it is positive. $\mathbf{e}_0 = [0, 0, 0, 1]^T$ in Eq.(2) is called *ideal plane* in which the corresponding projective distance does not depend on the Euclidean position of \mathbf{r} .



(a) basis vectors form discrete projective 2D subspaces



(b) projective distances between origin and basis planes

Figure 1. Discrete projective subspaces

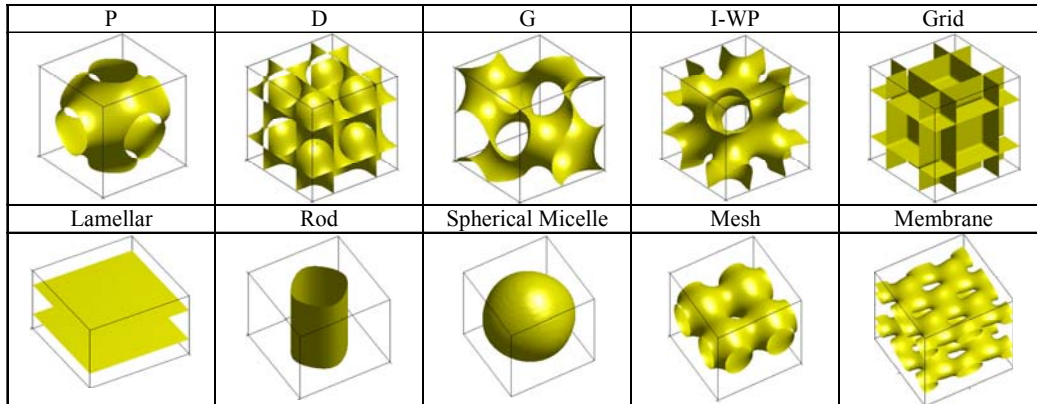


Figure 2. Periodic surface models of cubic phase and mesophase structures [2]

4. DEGREE ELEVATION

Degree elevation allows us to incrementally increase the complexity of models. Three types of degree elevation for periodic surfaces are studied here. They include the simplest native degree elevation, scale-dependent variational degree elevation, and constrained degree elevation with boundary conditions of continuity.

4.1 Native Degree Elevation

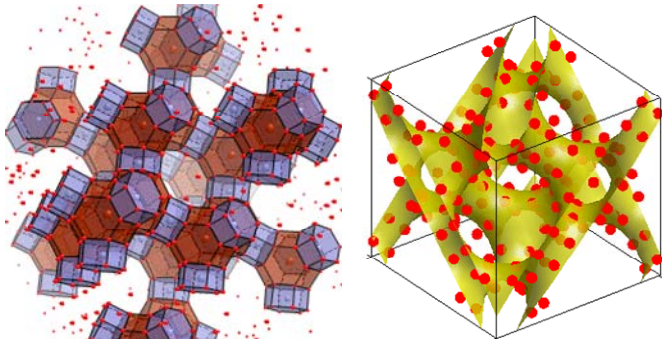
Because of the orthogonality of periodic basis functions, the native degree elevation of Eq. (1) is natural and trivial. It is to simply add new basis vectors with the corresponding moments that are all equal to zeros. That is,

$$\psi'(\mathbf{r}) = \sum_{l=1}^L \sum_{m=1}^{M+V} \mu_{lm} \cos(2\pi\kappa_l(\mathbf{p}_m^T \cdot \mathbf{r})) = 0 \quad (3)$$

where $\mu_{lm} = 0$ for all $l = 1, \dots, L$ and $m = M + 1, \dots, M + V$.

Example 1. Zeolites are known as molecular sieves that have porous structures of molecular dimensions. This allows small molecules such as water to pass through layers of sieves while bigger molecules are filtered out. Zeolites are widely applied for purification and separation as detergent, catalyst, and others. Figure 3 shows a loci PS model for one type of zeolites, Faujasite crystal. The PS model is

$$\begin{aligned} \psi(x, y, z) = & -0.50992 - 0.0098336 \cos(2\pi x) - 0.0098336 \cos(2\pi y) \\ & - 0.0098336 \cos(2\pi z) - 0.0042982 \cos(2\pi(x + y)) \\ & - 0.0042982 \cos(2\pi(x + z)) - 0.0042982 \cos(2\pi(y + z)) \\ & - 0.015304 \cos(2\pi(x - y)) - 0.015304 \cos(2\pi(z - x)) \\ & - 0.015304 \cos(2\pi(y - z)) - 0.45206 \cos(2\pi(x + y + z)) \\ & + 0.42213 \cos(2\pi(x - y + z)) + 0.42213 \cos(2\pi(y + z - x)) \\ & + 0.42213 \cos(2\pi(x + y - z)) = 0 \end{aligned}$$



(a) Faujasite crystal. Each tetradecahedron encloses a Fe, each hexagonal prism encloses an Al, and each vertex of the polygons represents a Si.

(b) Loci PS model of Si in Faujasite

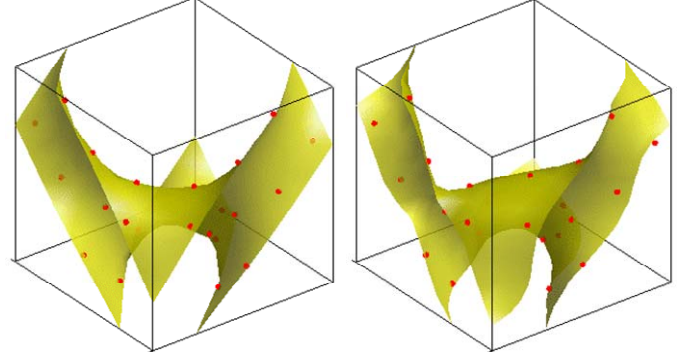
Figure 3. Loci PS model of Faujasite crystal

If 1/8 of the model in Figure 3-(b) is considered, we can have a zoom-in view of the model as in Figure 4-(a). When we need a more detailed control during the process of design so that the positions of atoms can be fine-tuned, the degree

elevation operation can provide the needs. Introducing three more basis vectors with the corresponding moments as zeros, we have more control on the surface model. Modifying the moments further we can create a different design, such as

$$\begin{aligned} \psi'(x, y, z) = & \psi(x, y, z) - 0.1 \cos(2\pi(x - 3y - z)) \\ & + 0.1 \cos(2\pi(y - x - 3z)) - 0.1 \cos(2\pi(z - 3x - y)) = 0 \end{aligned}$$

The new surface model is shown in Figure 4-(b).



(a) Original loci PS model $\psi(\mathbf{r})$

(b) An example of the elevated PS model $\psi'(\mathbf{r})$ to support detailed modifications

Figure 4. An example of degree elevation to support fine-tuned modification of the Faujasite PS model

4.2 Variational Degree Elevation

There exists no general scale-independent degree elevation such that

$$\forall \mathbf{r} \in \mathbb{P}^3, \quad (4)$$

$$\sum_{m=1}^M \mu_{lm} \cos(2\pi\kappa_l(\mathbf{p}_m^T \cdot \mathbf{r})) = \sum_{n=1}^N \mu'_{ln} \cos(2\pi\kappa_l(\mathbf{p}'_n^T \cdot \mathbf{r}))$$

where $\{\mathbf{p}_m\} \neq \{\mathbf{p}'_n\}$, $\mu_{lm} \neq 0$ and $\mu'_{ln} \neq 0$ for all l, m, n , and $M, N < \infty$ at some scale κ .

Nevertheless, we can have approximated variational degree elevation that is scale-dependent. For some small $\Delta\mathbf{p}_m$'s,

$$\begin{aligned} \sum_{l=1}^L \sum_{m=1}^M \mu_{lm} \cos(2\pi\kappa_l((\mathbf{p}_m^T + \Delta\mathbf{p}_m^T) \cdot \mathbf{r})) \approx \\ \sum_{l=1}^L \sum_{m=1}^M \mu_{lm} \left[\cos(2\pi\kappa_l(\mathbf{p}_m^T \cdot \mathbf{r})) - \cos\left(2\pi\kappa_l\left(\mathbf{p}_m^T \cdot \mathbf{r} - \frac{1}{4\kappa_l}\right)\right) (\Delta\mathbf{p}_m^T \cdot \mathbf{r}) \right] \\ = \sum_{l=1}^L \sum_{m=1}^M \mu_{lm} \left[\cos(2\pi\kappa_l(\mathbf{p}_m^T \cdot \mathbf{r})) - \cos(2\pi\kappa_l(\mathbf{q}_m^T \cdot \mathbf{r})) (\Delta\mathbf{p}_m^T \cdot \mathbf{r}) \right] \end{aligned}$$

where $\mathbf{q}_m = (a_m, b_m, c_m, \theta_m - 1/(4\kappa_l w))$ is a scale-dependent translated \mathbf{p}_m . In a given domain \mathbb{D} , for any l and m , if we can find some small moments $\Delta\mu_{lm}$'s such that

$$\Delta\mu_{lm} = \max_{\forall \mathbf{r} \in \mathbb{D}} |\mu_{lm} (\Delta\mathbf{p}_m^T \cdot \mathbf{r})| \quad (5)$$

then the scale-dependent variational degree elevation is

$$\begin{aligned}
& \sum_{l=1}^L \sum_{m=1}^M \mu_{lm} \cos(2\pi\kappa_l(\mathbf{p}_m^T \cdot \mathbf{r})) \\
& \approx \sum_{l=1}^L \sum_{m=1}^M \mu_{lm} \cos(2\pi\kappa_l((\mathbf{p}_m^T + \Delta\mathbf{p}_m^T) \cdot \mathbf{r})) \\
& + \sum_{l=1}^L \sum_{m=1}^M \Delta\mu_{lm} \cos(2\pi\kappa_l(\mathbf{q}_m^T \cdot \mathbf{r}))
\end{aligned} \tag{6}$$

For a given domain \mathbb{D} , the largest projective distances occur at the vertices of \mathbb{D} . As illustrated in Figure 5, the largest $\Delta\mathbf{p}_m^T \cdot \mathbf{r}$ always occurs at the corner points. Thus the lower and upper bounds of $\Delta\mu_{lm}$'s can easily be estimated.

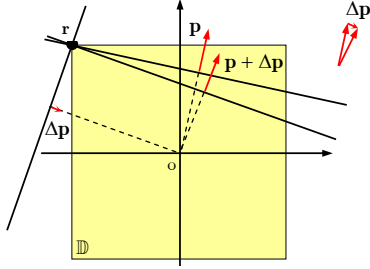


Figure 5. The lower and upper bounds of $\Delta\mu_{lm}$ are estimated at vertices of domains

Example 2. P surfaces can be used to build cage-like structures, such as Sodalite minerals, as shown in Figure 6. In the standard unit domain

$$\mathbb{D}_0 := \{(x, y, z, 1) \mid 0 \leq x \leq 1; 0 \leq y \leq 1; 0 \leq z \leq 1\} \tag{7}$$

an example of variational degree elevation of a standard P surface with the scale parameter $\kappa = 1$ and moments $\mu_1 = \mu_2 = \mu_3 = 1$ can be obtained as follows. The basis vectors are $\mathbf{p}_1 = [1, 0, 0]^T$, $\mathbf{p}_2 = [0, 1, 0]^T$, and $\mathbf{p}_3 = [0, 0, 1]^T$. Suppose the vector deviations are $\Delta\mathbf{p}_1 = [0.001, 0, 0]^T$, $\Delta\mathbf{p}_2 = [0.001, 0.001, 0]^T$, and $\Delta\mathbf{p}_3 = [0.001, 0.001, 0.001]^T$. It is not hard to find $\Delta\mu_1 = 0.001$, $\Delta\mu_2 = 0.002$, and $\Delta\mu_3 = 0.003$. With different vector deviations $\Delta\mathbf{p}_j$ ($j = 1, 2, 3$), the original and elevated surfaces are compared in Figure 6.

Theorem 1. The variational degree elevation is an approximation with quadratic convergence.

Proof. For any l and m ,

$$\begin{aligned}
Q_{lm} &= \mu_{lm} \cos(2\pi\kappa_l(\mathbf{p}_m^T \cdot \mathbf{r})) - \left[\mu_{lm} \cos(2\pi\kappa_l((\mathbf{p}_m^T + \Delta\mathbf{p}_m^T) \cdot \mathbf{r})) \right. \\
& \quad \left. + \Delta\mu_{lm} \cos(2\pi\kappa_l(\mathbf{q}_m^T \cdot \mathbf{r})) \right] \\
&= \mu_{lm} \cos(2\pi\kappa_l(\mathbf{p}_m^T \cdot \mathbf{r})) \\
& \quad - \mu_{lm} \cos(2\pi\kappa_l(\mathbf{p}_m^T \cdot \mathbf{r})) \cos(2\pi\kappa_l(\Delta\mathbf{p}_m^T \cdot \mathbf{r})) \\
& \quad + \mu_{lm} \sin(2\pi\kappa_l(\mathbf{p}_m^T \cdot \mathbf{r})) \sin(2\pi\kappa_l(\Delta\mathbf{p}_m^T \cdot \mathbf{r})) \\
& \quad - \Delta\mu_{lm} \sin(2\pi\kappa_l(\mathbf{p}_m^T \cdot \mathbf{r}))
\end{aligned}$$

$$\begin{aligned}
&= \mu_{lm} \cos(2\pi\kappa_l(\mathbf{p}_m^T \cdot \mathbf{r})) [1 - \cos(\Delta\mathbf{p}_m^T \cdot \mathbf{r})] \\
& \quad + \sin(2\pi\kappa_l(\mathbf{p}_m^T \cdot \mathbf{r})) [\mu_{lm} \sin(2\pi\kappa_l(\Delta\mathbf{p}_m^T \cdot \mathbf{r})) - \Delta\mu_{lm}]
\end{aligned}$$

Since $\cos(x) = 1 - \frac{x^2}{2!} + \frac{x^4}{4!} + O(x^6)$ and $\sin(x) = x - \frac{x^3}{3!} + \frac{x^5}{5!} + O(x^7)$ when $x \rightarrow 0$,

$$\begin{aligned}
Q_{lm} &= \mu_{lm} \cos(2\pi\kappa_l(\mathbf{p}_m^T \cdot \mathbf{r})) \left[\frac{(\Delta\mathbf{p}_m^T \cdot \mathbf{r})^2}{2!} + O((\Delta\mathbf{p}_m^T \cdot \mathbf{r})^4) \right] \\
& \quad + \sin(2\pi\kappa_l(\mathbf{p}_m^T \cdot \mathbf{r})) \left[\mu_{lm} \left((\Delta\mathbf{p}_m^T \cdot \mathbf{r}) - \frac{(\Delta\mathbf{p}_m^T \cdot \mathbf{r})^3}{3!} \right) \right. \\
& \quad \left. - \mu_{lm} (\Delta\mathbf{p}_m^T \cdot \mathbf{r}) + O((\Delta\mathbf{p}_m^T \cdot \mathbf{r})^5) \right] \\
&= \mu_{lm} \left[\cos(2\pi\kappa_l(\mathbf{p}_m^T \cdot \mathbf{r})) \frac{(\Delta\mathbf{p}_m^T \cdot \mathbf{r})^2}{2!} \right. \\
& \quad \left. - \sin(2\pi\kappa_l(\mathbf{p}_m^T \cdot \mathbf{r})) \frac{(\Delta\mathbf{p}_m^T \cdot \mathbf{r})^3}{3!} \right] + O((\Delta\mathbf{p}_m^T \cdot \mathbf{r})^4) \\
&= \mu_{lm} \cos(2\pi\kappa_l(\mathbf{p}_m^T \cdot \mathbf{r})) \frac{(\Delta\mathbf{p}_m^T \cdot \mathbf{r})^2}{2} + O((\Delta\mathbf{p}_m^T \cdot \mathbf{r})^3)
\end{aligned}$$

□

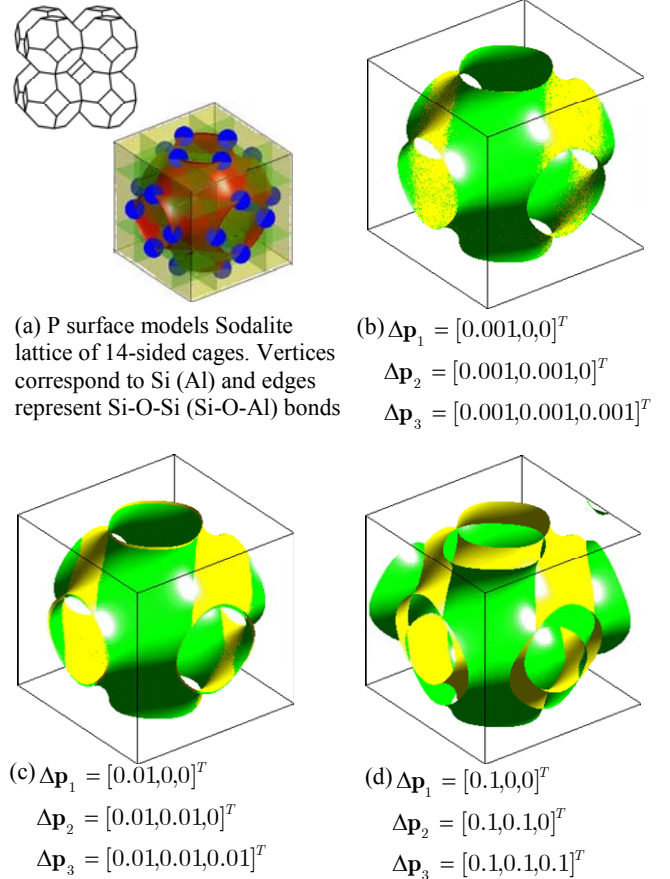
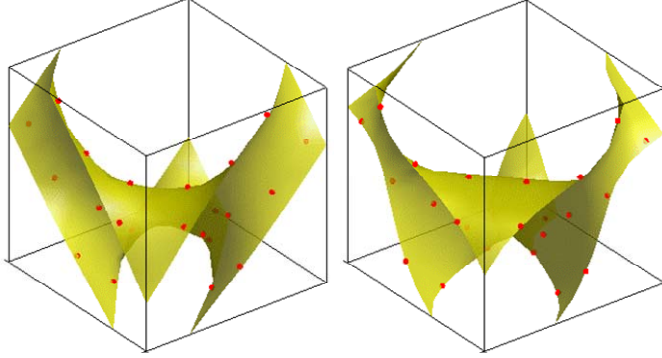


Figure 6. Examples of variational degree elevation of P surface, where the yellow surface is the original and the green is the elevated one

Example 3. We apply variational degree elevation to the Faujasite crystal model in Figure 3. The elevated surface is shown in Figure 7-(b), which has the form of

$$\begin{aligned} \psi^{11}(x, y, z) = & \psi(x, y, z) + 0.15 \cos(2\pi(1.1x + y + z - 0.25)) \\ & + 0.15 \cos(2\pi(1.1x - y + z - 0.25)) \\ & + 0.15 \cos(2\pi(y + z - 1.1x - 0.25)) \\ & + 0.15 \cos(2\pi(1.1x + y - z - 0.25)) = 0 \end{aligned}$$



(a) Original loci PS model $\psi(\mathbf{r})$ of Faujasite crystal

(b) The variationally elevated PS model $\psi^{11}(\mathbf{r})$

Figure 7. Variationally elevated surface model of the Faujasite crystal in Figure 3

4.3 Constrained Degree Elevation

In the future CAND systems, complex nanostructures are expected to be assembled based on some basic building blocks. Piecewise construction will be needed in the assembly process. To support piecewise construction of PS models, certain levels of surface continuity conditions may be required at the domain boundaries in degree elevation, which is called constrained degree elevation process. This can be achieved following the principles of shape approximation.

Theorem 2 [11]. If implicit surfaces $\sigma(\mathbf{r}) = 0$ and $\chi(\mathbf{r}) = 0$ intersect transversally in an irreducible curve $\gamma(\mathbf{r})$, then any algebraic surface $\eta(\mathbf{r}) = 0$ that meets $\sigma(\mathbf{r}) = 0$ with G^k rescaling continuity on $\gamma(\mathbf{r})$ must be in the form $\eta(\mathbf{r}) = \alpha(\mathbf{r})\sigma(\mathbf{r}) + \beta(\mathbf{r})\chi^{k+1}(\mathbf{r})$ where $\alpha(\mathbf{r})$ and $\beta(\mathbf{r})$ are polynomial functions that are not identically zero on $\gamma(\mathbf{r})$.

If considered in the standard unit domain \mathbb{D}_0 in Eq. (7), the periodic grid surface that defines the domain boundary is

$$\chi_g(\mathbf{r}) = \cos(2\pi\kappa_g(\mathbf{e}_x^T \cdot \mathbf{r}))\cos(2\pi\kappa_g(\mathbf{e}_y^T \cdot \mathbf{r}))\cos(2\pi\kappa_g(\mathbf{e}_z^T \cdot \mathbf{r}))$$

where $\mathbf{e}_x = [1, 0, 0, -1/2]^T$, $\mathbf{e}_y = [0, 1, 0, -1/2]^T$, $\mathbf{e}_z = [0, 0, 1, -1/2]^T$, and $\kappa_g = 1/2$. It is rewritten in the generic form as

$$\chi_g(\mathbf{r}) = \sum_{i=1}^4 \mu_g \cos(2\pi\kappa_g(\mathbf{e}_{g_i}^T \cdot \mathbf{r})) \quad (8)$$

where $\mathbf{e}_{g1} = [1, 1, 1, -3/2]^T$, $\mathbf{e}_{g2} = [1, 1, -1, -1/2]^T$, $\mathbf{e}_{g3} = [1, -1, 1, -1/2]^T$, $\mathbf{e}_{g4} = [1, -1, -1, 1/2]^T$, and $\mu_g = 1/4$.

Given a periodic zero surface $\psi(\mathbf{r}) = 0$, we can create a new surface $\psi^{(k)}(\mathbf{r}) = 0$ that meets with the original surface on the curve boundaries $\gamma(\mathbf{r}) = \psi^2(\mathbf{r}) + \chi_g^2(\mathbf{r}) = 0$ with G^k rescaling continuity as

$$\psi^{(k)}(\mathbf{r}) = \alpha(\mathbf{r})\psi(\mathbf{r}) + \beta(\mathbf{r})\chi_g^{k+1}(\mathbf{r}) \quad (9)$$

where periodic surfaces $\alpha(\mathbf{r})$ and $\beta(\mathbf{r})$ satisfy the condition $\exists \mathbf{r} \in \mathbb{D}_0, \gamma(\mathbf{r}) = 0, \alpha(\mathbf{r})\beta(\mathbf{r}) \neq 0$.

Example 4. An example of constrained degree elevation of P surface with G^0 continuity on unit boundary is surface

$$\begin{aligned} \psi^{(0)}(x, y, z) = & \alpha \{ \cos(2\pi(x)) + \cos(2\pi(y)) + \cos(2\pi(z)) \} \\ & + \beta \left\{ \begin{aligned} & 0.25 \cos(2\pi(0.5x + 0.5y + 0.5z - 0.75)) \\ & + 0.25 \cos(2\pi(0.5x + 0.5y - 0.5z - 0.25)) \\ & + 0.25 \cos(2\pi(0.5x - 0.5y + 0.5z - 0.25)) \\ & + 0.25 \cos(2\pi(0.5x - 0.5y - 0.5z + 0.25)) \end{aligned} \right\} \end{aligned}$$

An elevation with G^1 continuity results in surface

$$\begin{aligned} \psi^{(1)}(x, y, z) = & \alpha \{ \cos(2\pi(x)) + \cos(2\pi(y)) + \cos(2\pi(z)) \} \\ & + \beta \left\{ \begin{aligned} & 0.25 \cos(2\pi(0.5x + 0.5y + 0.5z - 0.75)) \\ & + 0.25 \cos(2\pi(0.5x + 0.5y - 0.5z - 0.25)) \\ & + 0.25 \cos(2\pi(0.5x - 0.5y + 0.5z - 0.25)) \\ & + 0.25 \cos(2\pi(0.5x - 0.5y - 0.5z + 0.25)) \end{aligned} \right\} \\ = & \alpha \{ \cos(2\pi(x)) + \cos(2\pi(y)) + \cos(2\pi(z)) \} \end{aligned}$$

$$\begin{aligned} & + \beta \left\{ \begin{aligned} & 0.125 + 0.03125 \cos(2\pi(x + y + z - 1.5)) \\ & + 0.03125 \cos(2\pi(x + y - z - 0.5)) \\ & + 0.03125 \cos(2\pi(x - y + z - 0.5)) \\ & + 0.03125 \cos(2\pi(x - y - z + 0.5)) \\ & + 0.0625 \cos(2\pi(x + y - 1)) + 0.0625 \cos(2\pi(z - 0.5)) \\ & + 0.0625 \cos(2\pi(x + z - 1)) + 0.0625 \cos(2\pi(y - 0.5)) \\ & + 0.0625 \cos(2\pi(x + 0.5)) + 0.0625 \cos(2\pi(y + z - 1)) \\ & + 0.0625 \cos(2\pi(x - 0.5)) + 0.0625 \cos(2\pi(y - z)) \\ & + 0.0625 \cos(2\pi(x - z)) + 0.0625 \cos(2\pi(y - 0.5)) \\ & + 0.0625 \cos(2\pi(x - y)) + 0.0625 \cos(2\pi(z - 0.5)) \end{aligned} \right\} \end{aligned}$$

as compared in Figure 8-(a) and Figure 8-(b).

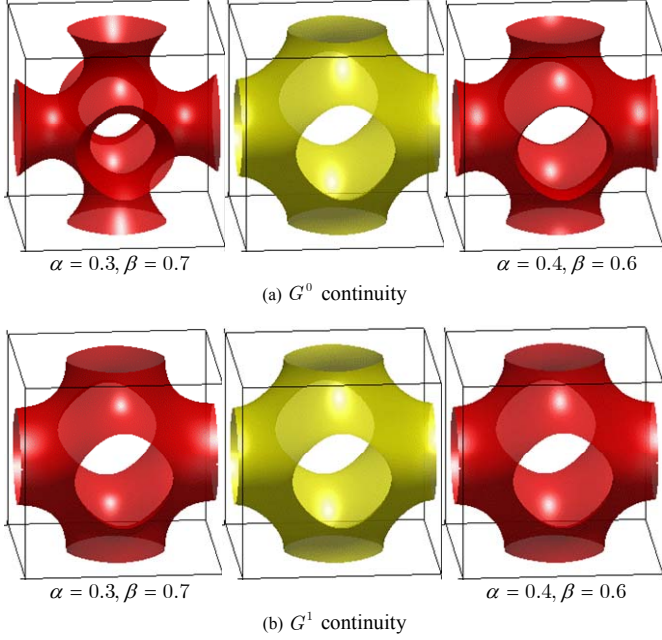


Figure 8. Examples of constrained degree elevation of P surface with G^0 and G^1 continuities, where yellow surfaces are the original P surfaces and red surfaces are the elevated ones

Example 5. A polymer morphological model

$$\begin{aligned}
\psi(x, y, z) = & -0.28087 + 0.32754 \cos(2\pi x) + 0.34605 \cos(2\pi y) \\
& - 0.29134 \cos(2\pi z) - 0.15175 \cos(2\pi(x + y)) \\
& + 0.44849 \cos(2\pi(x + z)) - 0.043878 \cos(2\pi(y + z)) \\
& - 0.10382 \cos(2\pi(x - y)) + 0.098657 \cos(2\pi(z - x)) \\
& + 0.19572 \cos(2\pi(y - z)) - 0.16861 \cos(2\pi(x + y + z)) \\
& - 0.28233 \cos(2\pi(x - y + z)) + 0.15767 \cos(2\pi(y + z - x)) \\
& - 0.16947 \cos(2\pi(x + y - z)) - 0.24857 \cos(4\pi x) \\
& - 0.037011 \cos(4\pi y) + 0.064369 \cos(4\pi z) \\
& - 0.043344 \cos(4\pi(x + y)) - 0.17759 \cos(4\pi(x + z)) \\
& - 0.098227 \cos(4\pi(y + z)) + 0.18506 \cos(4\pi(x - y)) \\
& - 0.0018576 \cos(4\pi(z - x)) + 0.074351 \cos(4\pi(y - z)) \\
& + 0.086133 \cos(4\pi(x + y + z)) - 0.056621 \cos(4\pi(x - y + z)) \\
& + 0.030192 \cos(4\pi(y + z - x)) + 0.029781 \cos(4\pi(x + y - z)) \\
= & 0
\end{aligned}$$

as shown in Figure 9-(b) is elevated with boundary continuity constraints. Following Eq. (9), we can construct two elevated PS models with G^0 and G^0 continuity as shown in Figure 9-(a) and Figure 9-(c) respectively.

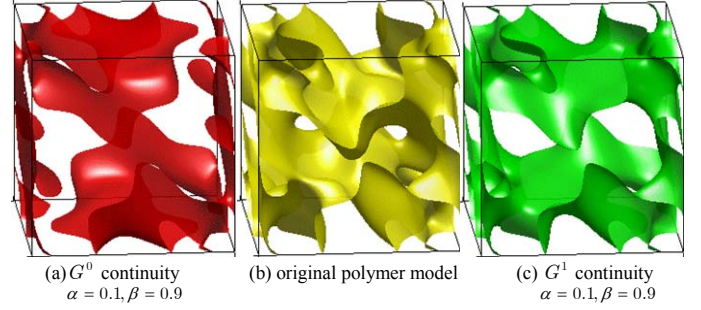


Figure 9. A polymer PS model with constrained degree elevations

5. DEGREE REDUCTION

Degree reduction is the reverse operation of degree elevation. When the complexity of a PS model needs to be reduced, the degree reduction operation derives a coarse-grained model with a lower resolution.

For a surface of Eq. (1), degree reduction in a domain \mathbb{D} is to find a

$$\psi'(\mathbf{r}) = \sum_{l=1}^L \sum_{n=1}^N \mu'_{ln} \cos(2\pi \kappa_l (\mathbf{p}'_n \cdot \mathbf{r}))$$

where $N < M$ such that the *algebraic distance* of the two surfaces

$$\text{dist}(\psi, \psi') := \iiint_{\mathbb{D}} [\psi(\mathbf{r}) - \psi'(\mathbf{r})]^2 d\mathbf{r} \quad (10)$$

is minimized in a complete volumetric domain \mathbb{D} for both ψ and ψ' .

$$\text{dist}(\psi, \psi') = \langle \psi(\mathbf{r}) - \psi'(\mathbf{r}), \psi(\mathbf{r}) - \psi'(\mathbf{r}) \rangle \quad (11)$$

$$= \sum_{l=1}^L \left\{ -2 \left\langle \sum_{m=1}^M \mu_{lm} \cos(2\pi \kappa_l (\mathbf{p}_m \cdot \mathbf{r})), \sum_{n=1}^N \mu'_{ln} \cos(2\pi \kappa_l (\mathbf{p}'_n \cdot \mathbf{r})) \right\rangle + \left\langle \sum_{n=1}^N \mu'_{ln} \cos(2\pi \kappa_l (\mathbf{p}'_n \cdot \mathbf{r})), \sum_{n=1}^N \mu'_{ln} \cos(2\pi \kappa_l (\mathbf{p}'_n \cdot \mathbf{r})) \right\rangle \right\}$$

Given a new set of periodic vectors $\{\mathbf{p}'_n\}$, the goal of degree reduction is to find optimal moments $\{\mu'_{ln}\}$ so that the distance in Eq. (10) is minimized. A necessary condition for the optimality is

$$\frac{\partial \text{dist}(\psi, \psi')}{\partial \mu'_{ln}} = 0 \quad (\text{for } l = 1, \dots, L, n = 1, \dots, N) \quad (12)$$

That is,

$$\begin{pmatrix} 2\mu'_{ln} \langle \cos(2\pi\kappa_l(\mathbf{p}'_n \cdot \mathbf{r})), \cos(2\pi\kappa_l(\mathbf{p}'_n \cdot \mathbf{r})) \rangle \\ + \sum_{\substack{m=1 \\ m \neq n}}^N \mu'_{lm} \langle \cos(2\pi\kappa_l(\mathbf{p}'_m \cdot \mathbf{r})), \cos(2\pi\kappa_l(\mathbf{p}'_n \cdot \mathbf{r})) \rangle \\ - 2 \sum_{m=1}^M \mu_{lm} \langle \cos(2\pi\kappa_l(\mathbf{p}_m^T \cdot \mathbf{r})), \cos(2\pi\kappa_l(\mathbf{p}'_n \cdot \mathbf{r})) \rangle \end{pmatrix} = 0 \quad (13)$$

(for $l = 1, \dots, L, n = 1, \dots, N$)

Thus, the problem of deriving optimal moments is reduced to solving L linear equation systems

$$[a_{lm}]_{N \times N} [\mu'_{ln}]_{N \times 1} = [b_{ln}]_{N \times 1} \quad (\text{for } l = 1, \dots, L) \quad (14)$$

where

$$a_{lm} = \begin{cases} \frac{1}{2} \langle \cos(2\pi\kappa_l(\mathbf{p}'_m \cdot \mathbf{r})), \cos(2\pi\kappa_l(\mathbf{p}'_n \cdot \mathbf{r})) \rangle & (\text{if } m \neq n) \\ \langle \cos(2\pi\kappa_l(\mathbf{p}'_n \cdot \mathbf{r})), \cos(2\pi\kappa_l(\mathbf{p}'_n \cdot \mathbf{r})) \rangle & (\text{if } m = n) \end{cases} \quad (15)$$

and

$$b_{ln} = \sum_{m=1}^M \mu_{lm} \langle \cos(2\pi\kappa_l(\mathbf{p}_m^T \cdot \mathbf{r})), \cos(2\pi\kappa_l(\mathbf{p}'_n \cdot \mathbf{r})) \rangle \quad (16)$$

Example 6. Surface

$$\begin{aligned} \psi_1(x, y, z) = & \cos(2\pi(-x + y + 0.25)) + \cos(2\pi(-x - y + 0.25)) \\ & + \cos(2\pi(-y + z + 0.25)) + \cos(2\pi(-y - z + 0.25)) \\ & + \cos(2\pi(x - z + 0.25)) + \cos(2\pi(-x - z + 0.25)) \\ & + 0.5 \cos(2\pi(5x)) + 0.5 \cos(2\pi(5y)) + 0.5 \cos(2\pi(5z)) \end{aligned}$$

which contains detailed features is reduced to a G-surface

$$\begin{aligned} \psi_{g1}(x, y, z) = & \cos(2\pi(-x + y + 0.25)) + \cos(2\pi(-x - y + 0.25)) \\ & + \cos(2\pi(-y + z + 0.25)) + \cos(2\pi(-y - z + 0.25)) \\ & + \cos(2\pi(x - z + 0.25)) + \cos(2\pi(-x - z + 0.25)) \end{aligned}$$

ψ_1 is shown in Figure 10-(a), and ψ_{g1} is in Figure 10-(b).

Surface

$$\begin{aligned} \psi_2(x, y, z) = & \cos(2\pi(-x + y + 0.25)) + \cos(2\pi(-x - y + 0.25)) \\ & + \cos(2\pi(-y + z + 0.25)) + \cos(2\pi(-y - z + 0.25)) \\ & + \cos(2\pi(x - z + 0.25)) + \cos(2\pi(-x - z + 0.25)) \\ & + \cos(2\pi(1.3x - 1.7y)) + \cos(2\pi(0.3y)) + \cos(2\pi(1.3z)) \end{aligned}$$

is also reduced to a G-surface

$$\begin{aligned} \psi_{g2}(x, y, z) = & 1.0387 \cos(2\pi(-x + y + 0.25)) \\ & + 1.2902 \cos(2\pi(-x - y + 0.25)) + \cos(2\pi(-y + z + 0.25)) \\ & + \cos(2\pi(-y - z + 0.25)) + \cos(2\pi(x - z + 0.25)) \\ & + \cos(2\pi(-x - z + 0.25)) \end{aligned}$$

ψ_2 is the yellow surface in Figure 11-(a), and ψ_{g2} is the blue surface in Figure 11-(b).

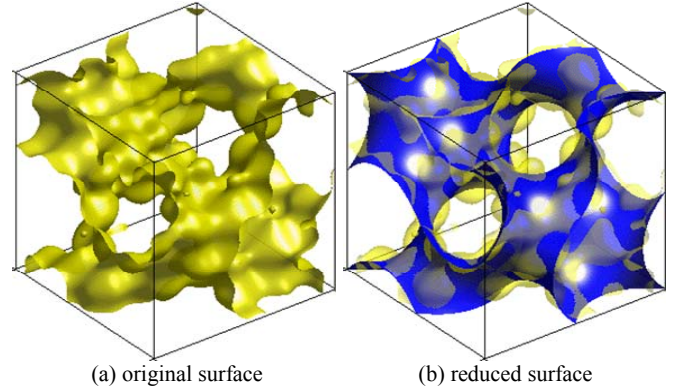


Figure 10. Degree reduction of surface ψ_1 where the original surface is in yellow and the reduced G-surface is in blue

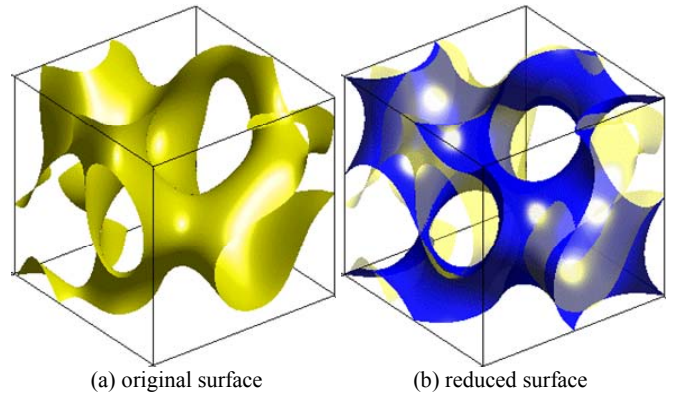


Figure 11. Degree reduction of surface ψ_2 where the original surface is in yellow and the reduced G-surface is in blue

Theorem 3. Based on the algebraic distance in Eq. (10), if the set of the new basis vectors $\{\mathbf{p}'_n\}$ is a subset of the original vectors $\{\mathbf{p}_m\}$, i.e., $\mathbf{p}'_n = \mathbf{p}_n$ ($n = 1, \dots, N$), and the basis vectors $\{\mathbf{p}_m\}$ are orthogonal to each other at the same scale in a domain \mathbb{D} , then degree reduction in \mathbb{D} is simply to extract the corresponding subset of moments $\mu'_n = \mu_n$ ($n = 1, \dots, N$).

Proof. From Eq. (15), because of the orthogonality, for any given scale l , we have

$$a_{lm} = \begin{cases} 0 & (\text{if } m \neq n) \\ \langle \cos(2\pi\kappa_l(\mathbf{p}_n^T \cdot \mathbf{r})), \cos(2\pi\kappa_l(\mathbf{p}_n^T \cdot \mathbf{r})) \rangle & (\text{if } m = n) \end{cases},$$

similarly, from Eq. (16), we have $b_{ln} = \mu_{ln} \langle \cos(2\pi\kappa_l(\mathbf{p}_n^T \cdot \mathbf{r})), \cos(2\pi\kappa_l(\mathbf{p}_n^T \cdot \mathbf{r})) \rangle$. Solving Eq. (14), we can derive $\mu'_{ln} = \mu_{ln}$ ($n = 1, \dots, N$).

□

Suppose there are K pairs of moments and periodic vectors that are common for both ψ and ψ' , that is, $\mu_{lm} = \mu'_{lm}$ and $\mathbf{p}_m = \mathbf{p}'_m$ for all $l = 1, \dots, L$ and $m = 1, \dots, K$.

It is easy to verify that

$$\sum_{l=1}^L \left\{ \begin{aligned} & \left\langle \sum_{m=1}^K \mu_{lm} \cos(2\pi\kappa_l(\mathbf{p}_m^T \cdot \mathbf{r})), \sum_{m=1}^K \mu_{lm} \cos(2\pi\kappa_l(\mathbf{p}_m^T \cdot \mathbf{r})) \right\rangle \\ & - 2 \left\langle \sum_{m=1}^K \mu_{lm} \cos(2\pi\kappa_l(\mathbf{p}_m^T \cdot \mathbf{r})), \sum_{n=1}^K \mu'_{ln} \cos(2\pi\kappa_l(\mathbf{p}_n^T \cdot \mathbf{r})) \right\rangle \\ & + \left\langle \sum_{n=1}^K \mu'_{ln} \cos(2\pi\kappa_l(\mathbf{p}_n^T \cdot \mathbf{r})), \sum_{n=1}^K \mu'_{ln} \cos(2\pi\kappa_l(\mathbf{p}_n^T \cdot \mathbf{r})) \right\rangle \end{aligned} \right\} = 0$$

Thus only those components that are different in either moments or periodic vectors in two surfaces contribute to the algebraic distance.

$\text{dist}(\psi, \psi') =$

$$\sum_{l=1}^L \left\{ \begin{aligned} & \left\langle \sum_{m=K+1}^M \mu_{lm} \cos(2\pi\kappa_l(\mathbf{p}_m^T \cdot \mathbf{r})), \sum_{m=K+1}^M \mu_{lm} \cos(2\pi\kappa_l(\mathbf{p}_m^T \cdot \mathbf{r})) \right\rangle \\ & - 2 \left\langle \sum_{m=K+1}^M \mu_{lm} \cos(2\pi\kappa_l(\mathbf{p}_m^T \cdot \mathbf{r})), \sum_{n=K+1}^N \mu'_{ln} \cos(2\pi\kappa_l(\mathbf{p}_n^T \cdot \mathbf{r})) \right\rangle \\ & + \left\langle \sum_{n=K+1}^N \mu'_{ln} \cos(2\pi\kappa_l(\mathbf{p}_n^T \cdot \mathbf{r})), \sum_{n=K+1}^N \mu'_{ln} \cos(2\pi\kappa_l(\mathbf{p}_n^T \cdot \mathbf{r})) \right\rangle \end{aligned} \right\}$$

If all pairs of basis vectors are identical but the corresponding moments are different, that is, $\mathbf{p}_m = \mathbf{p}'_m$ and $\mu_{lm} \neq \mu'_{lm}$ for all $l = 1, \dots, L$ and $m = K + 1, \dots, M$, then

$\text{dist}_{\parallel}(\psi, \psi') =$

$$\sum_{l=1}^L \sum_{m=K+1}^M (\mu_{lm} - \mu'_{lm})^2 \langle \cos(2\pi\kappa_l(\mathbf{p}_m^T \cdot \mathbf{r})), \cos(2\pi\kappa_l(\mathbf{p}_m^T \cdot \mathbf{r})) \rangle$$

If basis vectors \mathbf{p}_m 's and \mathbf{p}'_n 's are all orthogonal to each other at every scale l in \mathbb{D} , then

$\text{dist}_{\perp}(\psi, \psi') =$

$$\sum_{l=1}^L \left\{ \begin{aligned} & \sum_{m=K+1}^M \mu_{lm}^2 \langle \cos(2\pi\kappa_l(\mathbf{p}_m^T \cdot \mathbf{r})), \cos(2\pi\kappa_l(\mathbf{p}_m^T \cdot \mathbf{r})) \rangle \\ & + \sum_{n=K+1}^N \mu'_{ln}{}^2 \langle \cos(2\pi\kappa_l(\mathbf{p}_n^T \cdot \mathbf{r})), \cos(2\pi\kappa_l(\mathbf{p}_n^T \cdot \mathbf{r})) \rangle \end{aligned} \right\}$$

6. CONCLUDING REMARKS

Degree elevation and reduction operations are two basic mechanisms to control complexity of surface models in multi-resolution representation. In this paper, we study degree operations of periodic surfaces based on a generalized model. Three types of degree elevation are analyzed, including native degree elevation, scale-dependent variational degree elevation, and constrained degree elevation with boundary conditions. A degree reduction method is also developed based on an algebraic distance measurement.

ACKNOWLEDGEMENT

This work is supported in part by the NSF grant CMMI-0645070.

REFERENCES

- [1] Wang, Y. (2006) Geometric modeling of nano structures with periodic surfaces. *Lecture Notes in Computer Science*, Vol.4077, pp.343-356
- [2] Wang, Y. (2007) Periodic surface modeling for Computer Aided Nano Design. *Computer-Aided Design*, **39**(3): 179-189
- [3] Wang, Y. (2007) Loci periodic surface reconstruction from crystals. *Computer-Aided Design & Applications*, **4**(1-4): 437-447
- [4] Connolly, M.L. (1996) Molecular Surfaces: A Review. *Network Science*, Available at <http://www.netsci.org/Science/Compchem/index.html>
- [5] Lee, B. and Richards, F.M. (1971) The interpretation of protein structures: Estimation of static accessibility. *J. Mol. Biol.*, **55**: 379-400
- [6] Connolly, M.L. (1983) Solvent-accessible surfaces of proteins and nucleic acids. *Science*, **221**(4612): 709-713
- [7] Carson, M (1996) Wavelets and molecular structure. *J. Comp. Aided Mol. Des.*, **10**: 273-283
- [8] Edelsbrunner, H. (1999) Deformable smooth surface design. *Discrete & Computational Geometry*, **21**: 87-115
- [9] Bajaj, C., Pascucci, V., Shamir, A., Holt, R., and Netravali, A. (2003), Dynamic Maintenance and Visualization of Molecular Surfaces. *Discrete Applied Mathematics*, **127**: 23-51
- [10] Ryu, J., Kim, D., Cho, Y., Park, R. and Kim, D.-S. (2005) Computation of molecular surface using Euclidean Voronoi Diagram. *Computer-Aided Design & Applications*, **2**(1-4): 439-448
- [11] Bajaj, C., Ihm, I., and Warren, J. (1993) High-order interpolation and least-squares approximation using implicit algebraic surfaces. *ACM Trans. Graphics*, **12**(4): 327-347